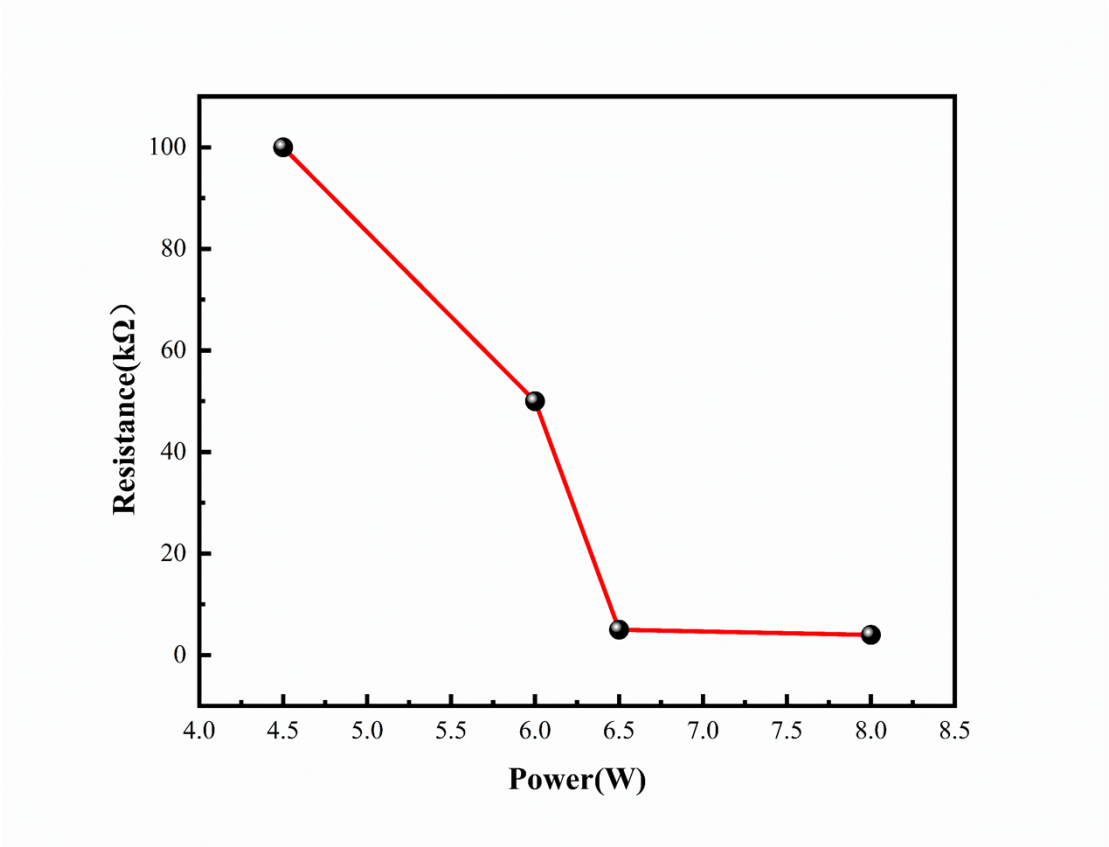

Figure S1. Electrical resistance of this sensor at different laser powers.

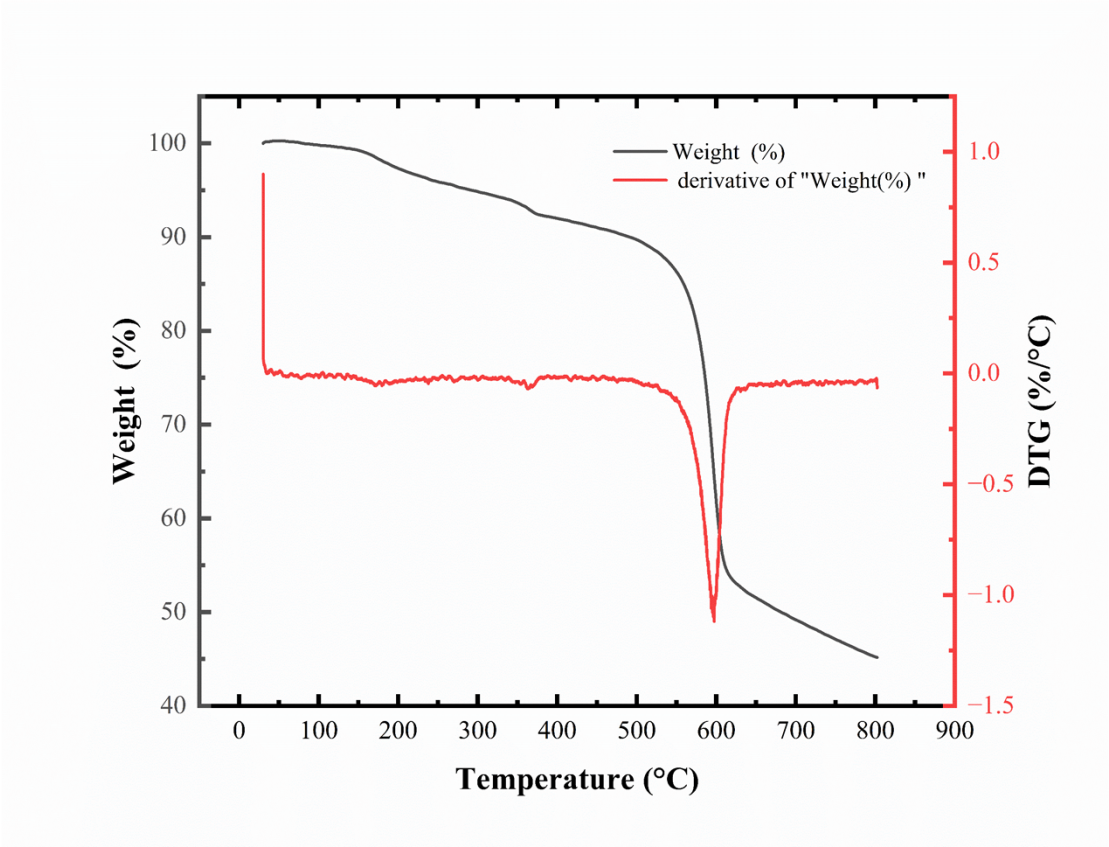

Figure S2. Thermogravimetric analysis (TGA) and derivative thermogravimetry (DTG) curves of the sensor.

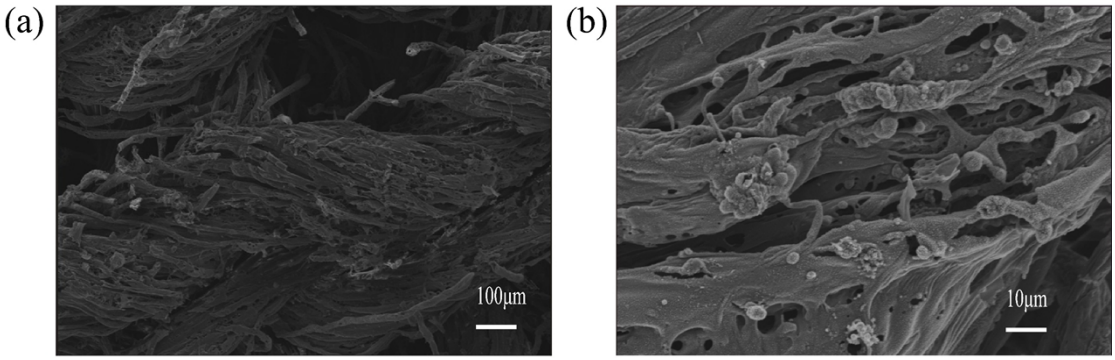

Figure S3. SEM images of the LIG(PI)/Kevlar sensor after 1000 stretching-releasing cycles at 6% strain. (a) Low-magnification and (b) high-magnification images.

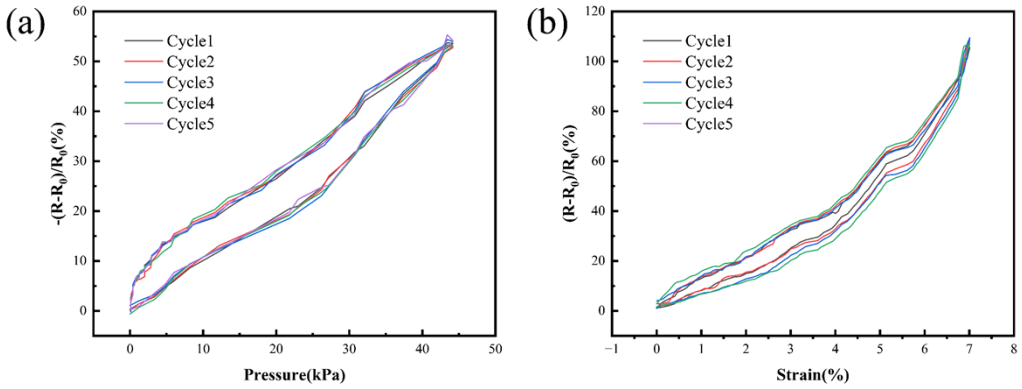

Figure S4. (a)Pressure hysteresis curves of the sensor. (b) Strain hysteresis curves of the sensor.

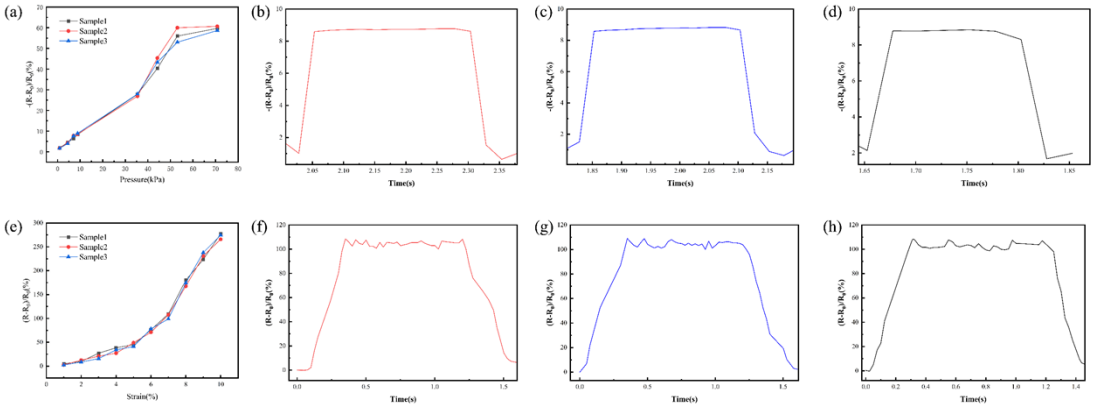

Figure S5. Evaluation of device uniformity and batch consistency. (a) Pressure sensitivity curves of three randomly selected sensors. (b-d) Real-time relative resistance variations of Sample 1, Sample 2, and Sample 3 under identical compressive loading, respectively. (e) Strain sensitivity curves of the three sensors. (f-h) Real-time relative resistance variations of Sample 1, Sample 2, and Sample 3 under identical tensile strain, respectively.

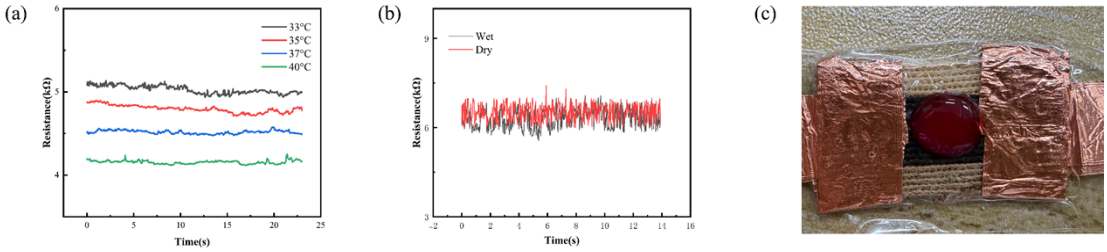

Figure S6. Stability tests of the sensor under different environmental conditions. (a) Resistance variations at different temperatures (33°C to 40°C). (b) Comparison of resistance signals in dry and wet conditions. (c) Photograph of the PU-encapsulated sensor during the water droplet test (using red-dyed water for visibility).